Chapter 1
Energy Consumption Analysis and Vehicle Power Demand

Energy saving technology is one of the most important research directions in the automotive industry [1–4]. For the major auto companies, it has significant influence to develop new products, enhance competitiveness and own their initiative in the market. In this chapter, on one hand, the actual vehicle energy consumption characteristics are analyzed with the visual graphics. On the other hand, the guidance about how the hybrid vehicle can save energy by the hybrid technology is given. On the basis of the above analysis, a practical solution based on the acceleration capability is proposed to calculate vehicle power demand directly.

1.1 Energy Consumption Analysis

The conventional vehicle has only one power source, i.e. the engine. The engine power must satisfy the requirement of the maximum velocity, the gradeability and the acceleration capability. To meet the dynamic requirements, the maximum power of engine could be 10 times as large as the power demand which the vehicle need when cruising on the horizontal road at speed of 100 km/h, or 3–4 times as at 6% grade at the speed of 100 km/h [5]. The inherent shortcomings of the single power source of the traditional vehicle create the energy consumption characteristics, which are of guiding significance to the research of the hybrid vehicle.

In this section, based on the fact that the conventional vehicle has poor fuel consumption performance, a visual and effective method on different driving cycles is proposed to analyze the fuel consumption characteristics. Then, an energy saving design method is given.

X. Zeng and J. Wang, *Analysis and Design of the Power-Split Device for Hybrid Systems*, https://doi.org/10.1007/978-981-10-4272-0_1

1.1.1 Energy Consumption

In this section, the representative driving cycles, including China Car Driving Cycle (CCDC), New European Driving Cycle (NEDC), the Japanese 10–15 Driving Cycle (10–15) and Urban Dynamometer Driving Schedule (UDDS), are chosen to analyze energy consumption.

1.1.1.1 Parameters of Conventional Vehicle

Table 1.1 shows the parameters of a conventional vehicle. This conventional vehicle has a 64 kW 4-cylinder engine. Its 0–100 km/h acceleration time is 16.6 s and the maximum velocity is 180 km/h.

1.1.1.2 Fuel Consumption of Conventional Vehicle

Simulation model for the conventional vehicle is established. After simulating under the driving cycles mentioned above, the fuel consumption results are shown in Table 1.2.

According to the data in Table 1.2, some differences in fuel consumption under different driving cycles can be seen. The fuel consumption under 10–15 driving cycle is the maximum while that under the NEDC is the minimum. Overall, this conventional vehicle consumes much fuel under all of the driving cycles and the average fuel consumption is 7.5 L/100 km.

The fuel consumption of traditional vehicle should be analyzed not only from the amount of fuel consumption, but also from the characteristics of fuel consumption, which can provide a solution for further improving the vehicle fuel economy.

Table 1.1 Parameters of a conventional vehicle

Vehicle parameters	Mass/kg	1500
	Transmission	5-Manual
Engine parameters	[Maximum power/kW]/[Speed/rpm]	64/6000
	[Peak torque/Nm]/[Speed/rpm]	120/4200

Table 1.2 Fuel consumption of the conventional vehicle

Driving cycle	CCDC	NEDC	10–15	UDDS
Fuel consumption/L	7.6	7.0	8.1	7.2

1.1.2 Characteristics Analysis

The analysis of the characteristics of vehicle fuel consumption is mainly to study the distribution of engine operating points during vehicle driving, i.e. according to the simulation results of fuel consumption, the output speed, torque and fuel rate of the engine are investigated.

The early research on the distribution of engine operating points is mainly done according to the engine 2-dimensional distribution points [6–8], which can only get the distribution characteristics qualitatively and is difficult to analyze the proportion of the operating time and the proportion of fuel consumption on the engine MAP.

In this section, the distribution characteristics on the engine MAP is studied quantificationally based on the statistical analysis method.

(1) Study the time proportion of different engine operating points (area) and search for the time distribution of engine load.
(2) Study the accumulated fuel consumption of different engine operating points (area) and search for the main fuel consumption points (area).

The above quantitative analysis can provide more practical guidance for engine MAP design and vehicle energy savings by hybrid technology.

1.1.3 Statistical Analysis

The vehicle model established in ADVISOR is simulated under the different driving cycles mentioned above. Then, the distribution characteristics of the engine MAP is studied quantificationally based on the statistical analysis.

1.1.3.1 Statistical Analysis Under CCDC

Based on the driving cycle shown in Fig. 1.1, the engine MAP within its operating range and the operating points are shown in Fig. 1.2.

1. Analysis of the time proportion

According to the simulation results, the time proportion of engine operating points under CCDC is calculated and the operating time distribution is shown in Table 1.3 and Fig. 1.3 with the histogram.

2. Analysis of fuel proportion

The proportion of the engine accumulated fuel consumption in different areas under CCDC is shown in Table 1.4 and Fig. 1.4 with the histogram.

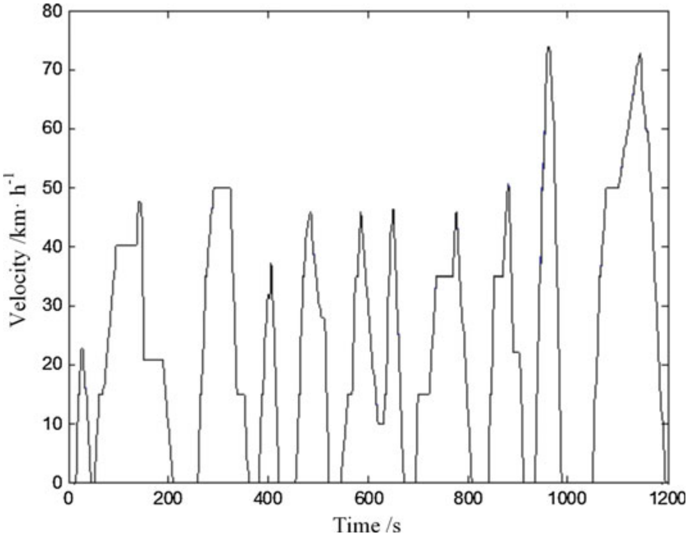

Fig. 1.1 Velocity-time curve of CCDC

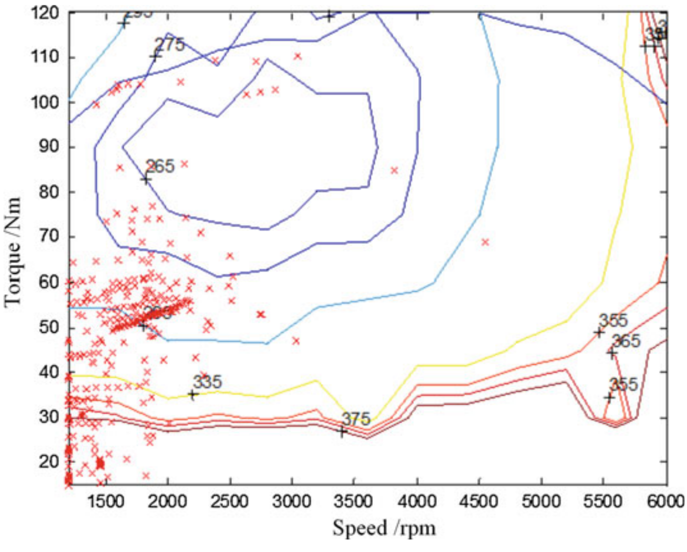

Fig. 1.2 Engine operating points under CCDC

Table 1.3 Operating time proportion under CCDC (%)

Speed/rpm	Torque/Nm						
	0	20	40	60	80	100	120
1200	22.1	36.8	28.5	6.8	0.7	2.0	0
2400	0	0	1.0	0.5	0	1.0	0
3600	0	0	0	0.2	0.2	0	0
4800	0	0	0	0	0	0	0
6000	0	0	0	0	0	0	0

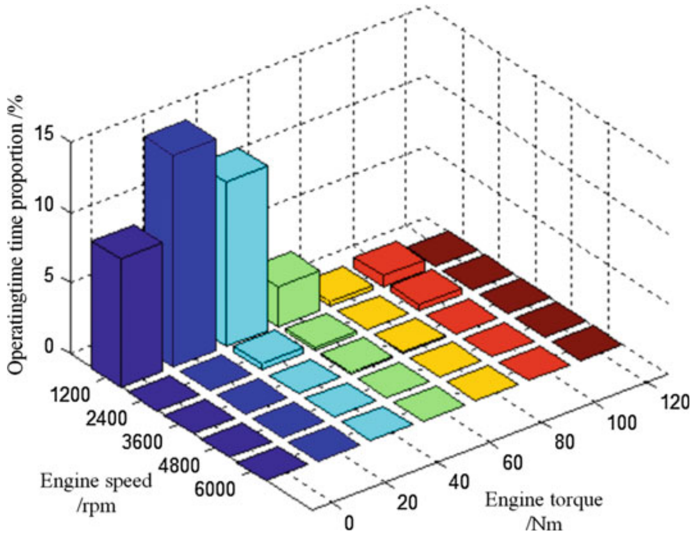

Fig. 1.3 Operating time proportion under CCDC

Table 1.4 Fuel proportion under CCDC (%)

Speed/rpm	Torque/Nm						
	0	20	40	60	80	100	120
1200	11.5	26.5	36.2	10.8	1.7	4.6	0
2400	0	0	2.1	1.0	0	3.8	0
3600	0	0	0	1.0	0.8	0	0
4800	0	0	0	0	0	0	0
6000	0	0	0	0	0	0	0

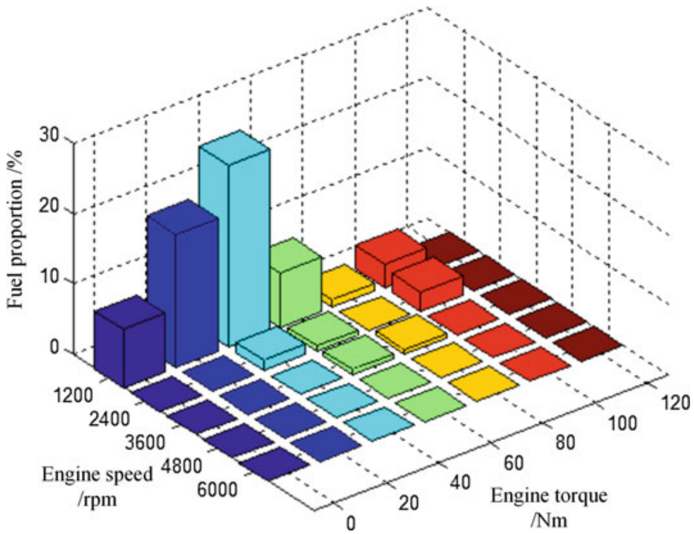

Fig. 1.4 Fuel proportion under CCDC

1.1.3.2 Statistical Analysis Under NEDC

Based on NEDC shown in Fig. 1.5, the distribution of engine operating points is shown in Fig. 1.6.

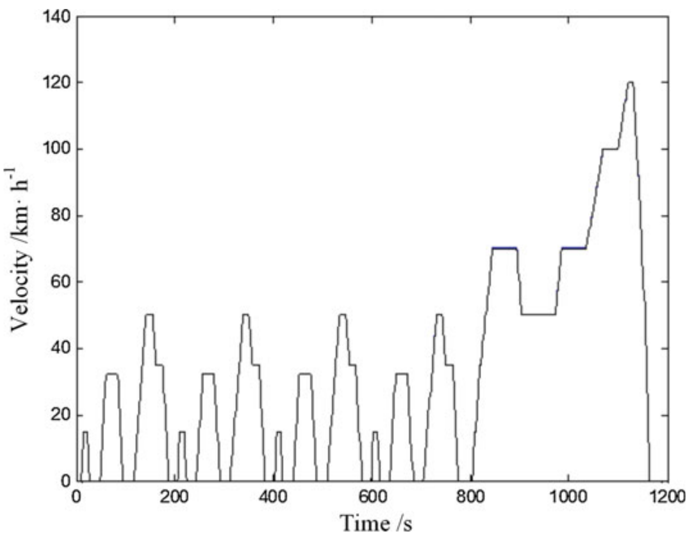

Fig. 1.5 Velocity-time curve of NEDC

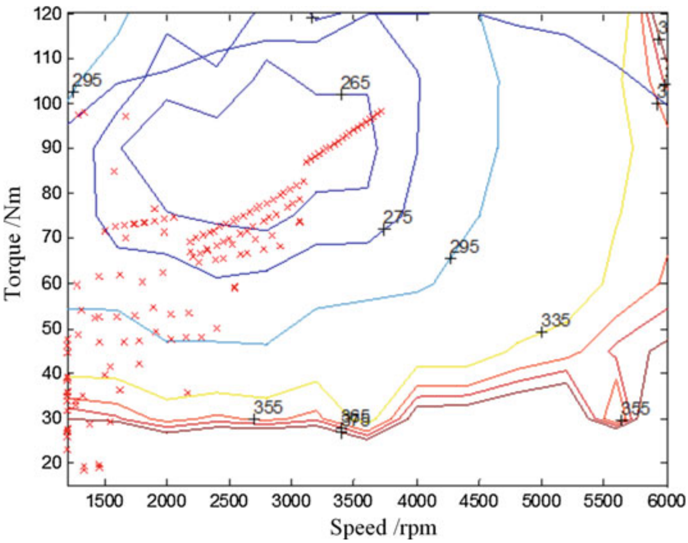

Fig. 1.6 Engine operating points under NEDC

Table 1.5 Operating time proportion under NEDC (%)

Speed/rpm	Torque/Nm						
	0	20	40	60	80	100	120
1200	17.9	28.5	25.9	10.1	0.6	0	0
2400	0	0	5.5	7.8	3.2	0	0
3600	0	0	0	0	0.6	0	0
4800	0	0	0	0	0	0	0
6000	0	0	0	0	0	0	0

1. Analysis of the time proportion

According to the simulation results, the time proportion of engine operating points under NEDC is calculated and the operating time distribution is shown in Table 1.5 and Fig. 1.7 with the histogram.

2. Analysis of fuel proportion

The proportion of the engine accumulated fuel consumption in different areas under NEDC is shown in Table 1.6 and Fig. 1.8 with the histogram.

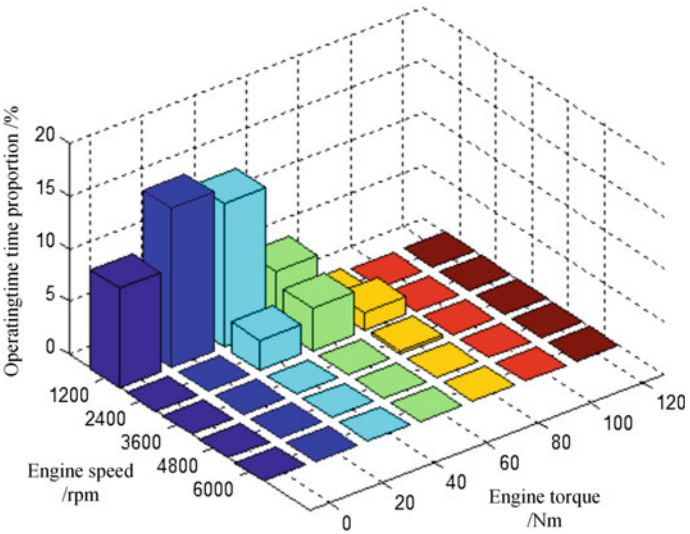

Fig. 1.7 Operating time proportion under NEDC

Table 1.6 Fuel proportion under NEDC (%)

Speed/rpm	Torque/Nm						
	0	20	40	60	80	100	120
1200	7.9	17.0	24.0	14.5	1.0	0	0
2400	0	0	8.5	15.6	9.3	3.8	0
3600	0	0	0	0	2.3	0	0
4800	0	0	0	0	0	0	0
6000	0	0	0	0	0	0	0

1.1.3.3 Statistical Analysis Under 10–15 Driving Cycle

Based on 10–15 driving cycle shown in Fig. 1.9, the distribution of engine operating points is shown in Fig. 1.10.

1. Analysis of the time proportion

According to the simulation results, the time proportion of engine operating points under 10–15 driving cycle is calculated and the operating time distribution is shown in Table 1.7 and Fig. 1.11 with the histogram.

2. Analysis of fuel proportion

The proportion of the engine accumulated fuel consumption in different areas under 10–15 driving cycle is shown in Table 1.8 and Fig. 1.12 with the histogram.

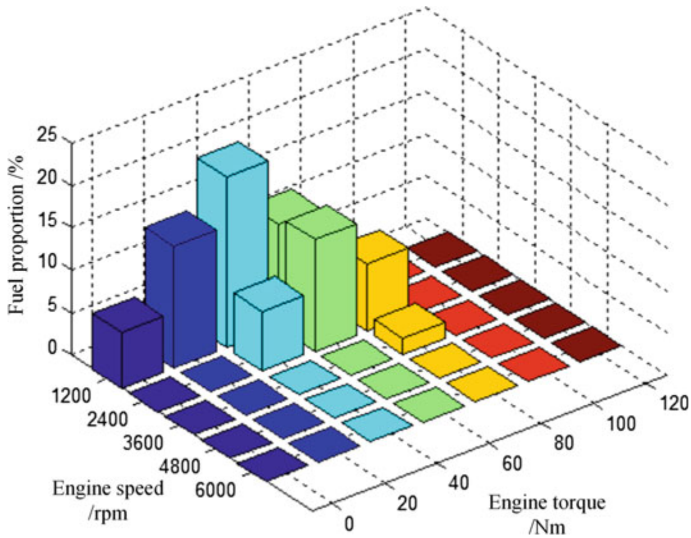

Fig. 1.8 Fuel proportion under NEDC

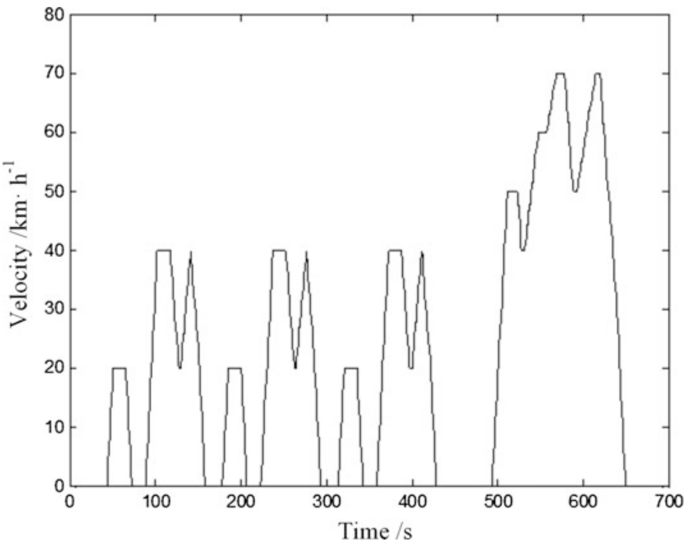

Fig. 1.9 Velocity-time curve of 10–15 driving cycle

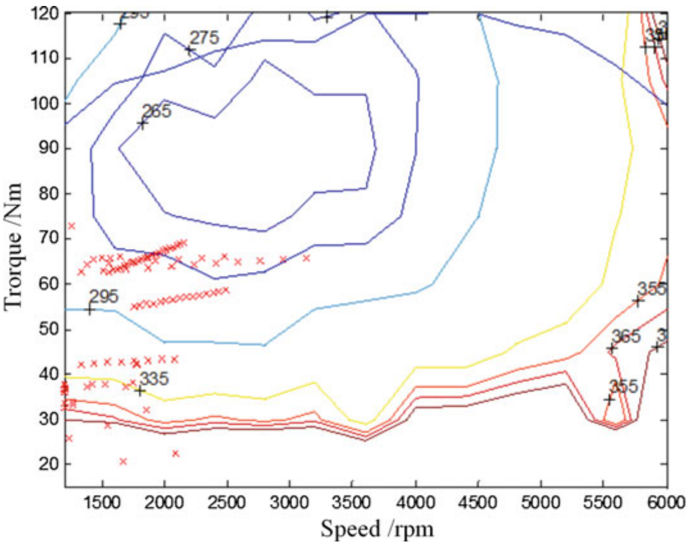

Fig. 1.10 Engine operating points under 10–15 driving cycle

Table 1.7 Operating time proportion under 10–15 driving cycle (%)

Speed/rpm	Torque/Nm						
	0	20	40	60	80	100	120
1200	17.6	38.0	17.6	23.6	0	0	0
2400	0	0	0.7	2.8	0	0	0
3600	0	0	0	0	0	0	0
4800	0	0	0	0	0	0	0
6000	0	0	0	0	0	0	0

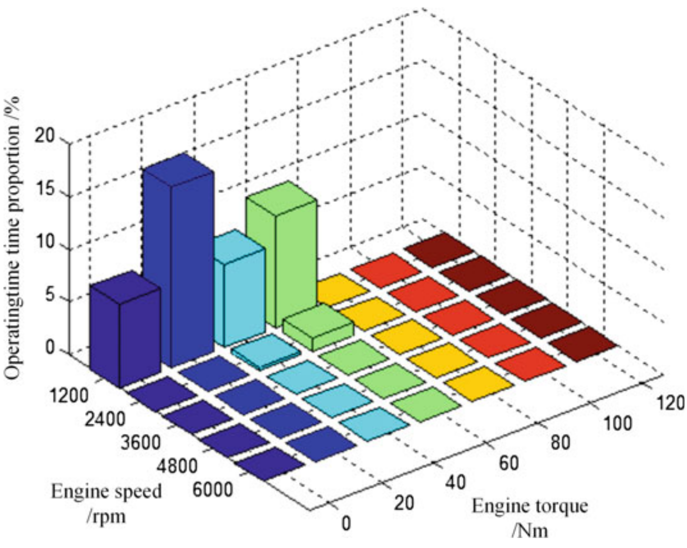

Fig. 1.11 Operating time proportion under 10–15 driving cycle

Table 1.8 Fuel proportion under 10–15 driving cycle (%)

Speed/rpm	Torque/Nm						
	0	20	40	60	80	100	120
1200	7.5	27.4	21.1	36.6	0	0	0
2400	0	0	1.3	6.1	0	0	0
3600	0	0	0	0	0	0	0
4800	0	0	0	0	0	0	0
6000	0	0	0	0	0	0	0

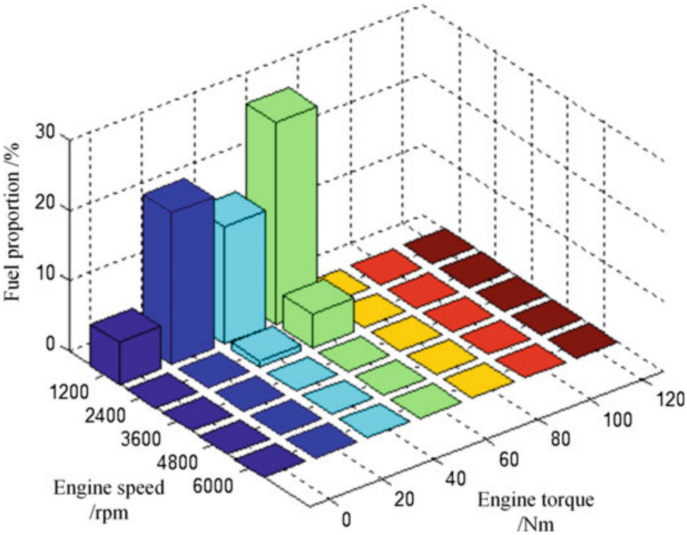

Fig. 1.12 Fuel proportion under 10–15 driving cycle

1.1.3.4 Statistical Analysis Under UDDS

Based on UDDS shown in Fig. 1.13, the distribution of engine operating points is shown in Fig. 1.14.

1. Analysis of the time proportion

According to the simulation results, the time proportion of engine operating points under UDDS is calculated and the operating time distribution is shown in Table 1.9 and Fig. 1.15 with the histogram.

2. Analysis of fuel proportion

The proportion of the engine accumulated fuel consumption in different areas under UDDS is shown in Table 1.10 and Fig. 1.16 with the histogram.

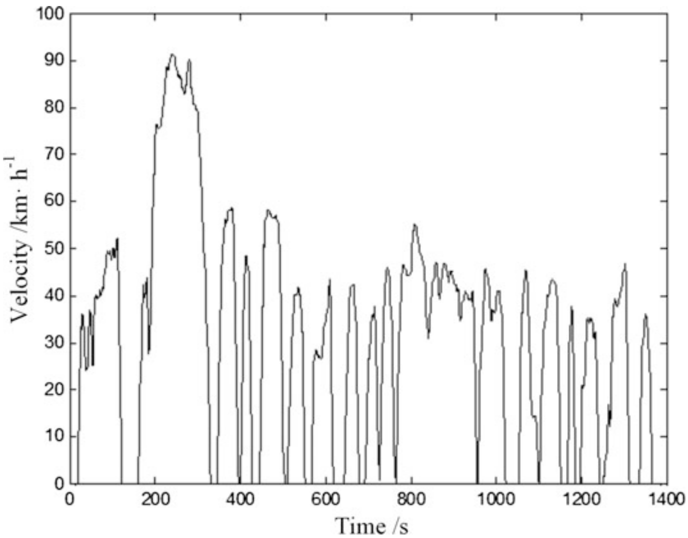

Fig. 1.13 Velocity-time curve of UDDS

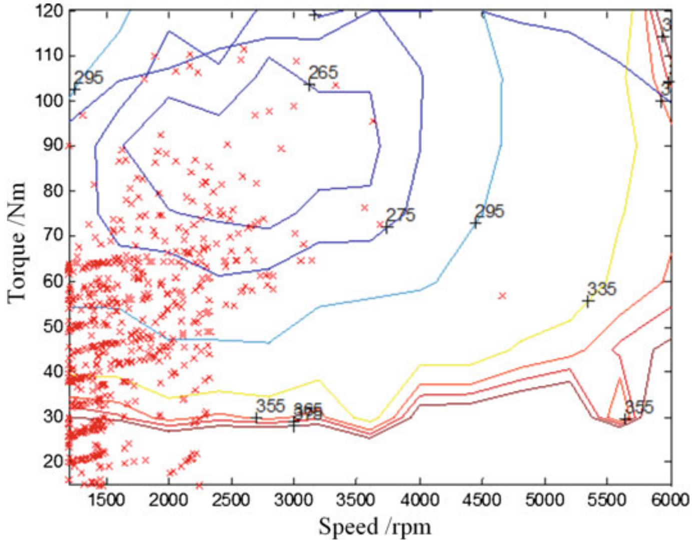

Fig. 1.14 Engine operating points under UDDS

1.1.3.5 Statistical Analysis Under Different Driving Cycles

The results based on the statistical analysis of fuel consumption characteristics under the above driving cycles show that the engine of conventional vehicle often works in low speed and low load area, which causes much fuel consumption.

Table 1.9 Operating time proportion under UDDS (%)

Speed/rpm	Torque/Nm						
	0	20	40	60	80	100	120
1200	15.7	28.2	29.2	16.2	2.8	0.9	0
2400	0	0	1.0	3.9	1.0	0.5	0
3600	0	0	0.2	0.2	0.2	0	0
4800	0	0	0	0	0	0	0
6000	0	0	0	0	0	0	0

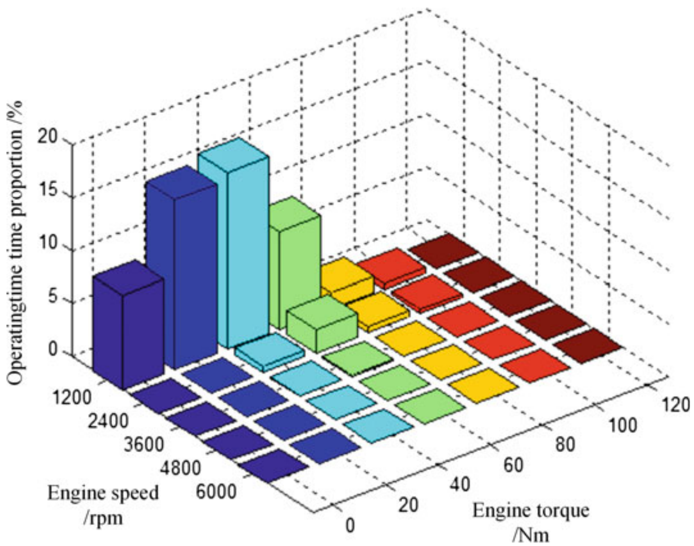

Fig. 1.15 Operating time proportion under UDDS

Table 1.10 Fuel proportion under UDDS (%)

Speed/rpm	Torque/Nm						
	0	20	40	60	80	100	120
1200	5.6	18.5	30.3	21.7	5.0	2.2	0
2400	0	0	1.9	8.4	2.9	1.9	0
3600	0	0	0.6	0.5	0.6	0	0
4800	0	0	0	0	0	0	0
6000	0	0	0	0	0	0	0

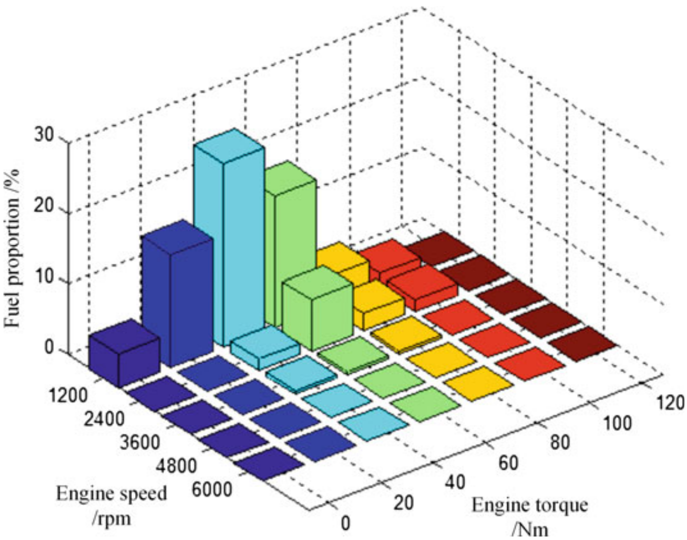

Fig. 1.16 Fuel proportion under UDDS

In the area which is enclosed by engine torque below 40 Nm (load factor is about 30%) and speed below 1200 rpm (20% of the maximum speed), the time proportion of engine operating points and fuel proportion under different driving cycles are shown in Tables 1.11, 1.12, 1.13 and 1.14.

Time proportion under CCDC is 87.4% and fuel consumption in this area is 74.2%.

Table 1.11 Analysis of engine operating points under low load (CCDC)

Speed/rpm	Torque/Nm			
	0–20		20–40	
	Time proportion/%	Fuel consumption proportion/%	Time proportion/%	Fuel consumption proportion/%
0–1200	58.9	38.0	28.5	36.2

Table 1.12 Analysis of engine operating points under low load (NEDC)

Speed/rpm	Torque/Nm			
	0–20		20–40	
	Time proportion/%	Fuel consumption proportion/%	Time proportion/%	Fuel consumption proportion/%
0–1200	46.4	24.9	25.9	24.0

Table 1.13 Analysis of engine operating points under low load (10–15 driving cycle)

Speed/rpm	Torque/Nm			
	0–20		20–40	
	Time proportion/%	Fuel consumption proportion/%	Time proportion/%	Fuel consumption proportion/%
0–1200	55.6	34.9	17.6	21.1

Table 1.14 Analysis of engine operating points under low load (UDDS)

Speed/rpm	Torque/Nm			
	0–20		20–40	
	Time proportion/%	Fuel consumption proportion/%	Time proportion/%	Fuel consumption proportion/%
0–1200	43.9	24.1	29.2	30.3

Time proportion under NEDC is 72.3% and fuel consumption in this area is 48.9%.

Time proportion under 10–15 driving cycle is 73.2% and fuel consumption in this area is 56.0%.

Time proportion under UDDS is 73.1% and fuel consumption in this area is 54.5%.

It can be seen that the time proportion of the engine under low load is very large. Although the fuel rate is not high in this area, the final calculated fuel consumption under low load is still large. Therefore, by choosing a smaller power engine, eliminating the idle or driving in pure electric mode in this area, the overall efficiency of the vehicle can be improved effectively, for example, by hybrid technology. This analysis method and results have practical value to improve vehicle fuel consumption and optimize the design of engine MAP.

1.2 Vehicle Power Demand

One of the cores for hybrid vehicle control is the appropriate power distribution between the two power sources, whose foundation is to find the solution for vehicle power demand. In this section, the traditional power calculation method is introduced. Then, in order to overcome its disadvantages, a reasonable and practical method to calculate the vehicle power demand directly based on the acceleration index is proposed.

1.2.1 Traditional Power Calculation Method

A traditional method to calculate vehicle power demand is usually an iterative, step-by-step method by simulation.

According to the maximum vehicle speed, the maximum vehicle power demand P_1 is calculated using the following equation [9]

$$P_1 = P_f + P_w = \frac{1}{3600 \cdot \eta_t} \left(m \cdot g \cdot f \cdot v + \frac{C_D \cdot A}{21.15} v^3 \right) \tag{1.1}$$

where P_f is the power of rolling resistance, P_w is the power of air resistance, C_D is the air resistance coefficient, A is frontal area, f is the rolling resistance coefficient, η_t is mechanical efficiency of the powertrain, m is total vehicle mass, g is gravitational acceleration and v is vehicle speed.

To ensure that the vehicle can meet the requirement of gradeability, the vehicle power demand P_2 at a particular speed at particular grade is calculated by

$$P_2 = P_f + P_w + P_i = \frac{1}{3600 \cdot \eta_t} \left(m \cdot \cos\theta \cdot g \cdot f \cdot v + \frac{C_D \cdot A}{21.15} v^3 + mg \cdot \sin\theta \cdot v \right) \tag{1.2}$$

where P_i is the power of grade resistance and θ is the road grade.

Finally, the larger value in P_1 and P_2 is used as the power demand, which cannot meet the demand of the extreme acceleration because it only considers the maximum velocity and climbing performance. So, generally, the following steps will be needed to ensure the vehicle power demand correctly:

(1) Set a maximum power and then match parameters of power sources of the hybrid vehicle.
(2) Establish models for the hybrid vehicle and simulate the acceleration time.
(3) If the acceleration time cannot meet the design demand, the power demand should be modified. Then, repeat step 1 and step 2 until meeting the design demand and the vehicle power demand is finally determined.

The traditional method to calculate vehicle power combines theory and simulation and is an iterative, step-by-step method. However, it is time consuming and not intuitive [7, 9, 10].

1.2.2 Practical Power Calculation Method and Application

To address the issue that the traditional method is not intuitive and also costs a long time, in this section, a preliminary method for calculating the power demand based on acceleration index is discussed. The theoretical equations of this method are deduced in detail, the impact coefficients in the equations are discussed and compared with the simulation curves of the vehicle acceleration process to verify the rationality and practicability of the method.

1.2.2.1 Practical Power Calculation Method

For most of the vehicles, the maximum power depends on the acceleration capability, which means once acceleration index is satisfied, other indices will be satisfied as well [10]. Simulation comparison between power demand of acceleration of a vehicle weighted 1000 kg and driving at a constant velocity (100 km/h) is shown in Fig. 1.17 and it can be seen that the power of acceleration is larger than power at constant velocity.

1.2.2.2 Theoretical Equations for Vehicle Acceleration Capability

When calculating the total power of power source, there are following assumptions:

(1) Characteristics curve for power source should be power contour (conventional vehicle with multi-gear transmission and electric vehicle (EV) both have external characteristics approximate to power contour).
(2) The rolling resistance and air resistance during acceleration are ignored (these road resistances are very small at low velocity).

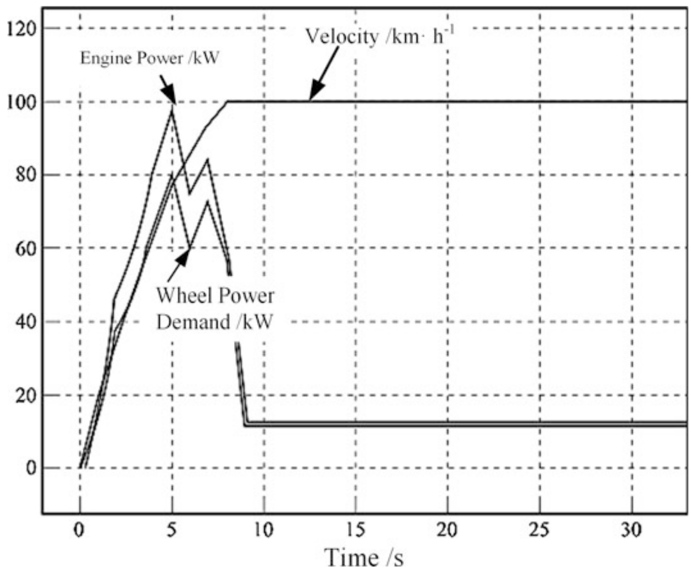

Fig. 1.17 Comparison of power demand between acceleration and constant velocity

Based on the above assumptions, vehicle kinetic equilibrium equation is shown as:

$$F \cdot v = P \rightarrow F = \frac{P}{v} \tag{1.3}$$

The power value P is set to a constant A and equation is derived as below:

$$a = \frac{F}{m} = \frac{dv}{dt} \xrightarrow{F(v)=A/v} \frac{A}{m \cdot v} = \frac{dv}{dt} \xrightarrow{B=A/m} B \cdot dt = v \cdot dv \tag{1.4}$$

$$\int_{0}^{t_m} Bdt = \int_{0}^{v_m} vdv \tag{1.5}$$

$$2B = \frac{v_m^2}{t_m} = \frac{v^2}{t} \rightarrow v = v_m \left(\frac{t}{t_m}\right)^{0.5} \tag{1.6}$$

So, vehicle speed could be approximated as [11]:

$$v = v_m \left(\frac{t}{t_m}\right)^{x} \tag{1.7}$$

where x is fitting coefficient, which is 0.5 generally; t_m, v_m are acceleration time and final velocity respectively; t is time; v is current velocity at time t; F, v are driving force of power source and velocity respectively; m is vehicle mass.

1.2.2.3 Impact Factors of Vehicle Acceleration Capacity

From last section, it can be seen that it's easy to estimate vehicle dynamic using Eq. (1.7) to represent velocity curves of acceleration. So what is the relationship between the real acceleration process and the factor x in Eq. (1.7)? It is the effect of x on the vehicle acceleration capacity that is the key to the question. Reference [12] makes a preliminary discussion and proposes that x should be about 0.47–0.53. Since the external characteristics of vehicle power source is approximate power contour, if vehicle has a better acceleration capacity, i.e. higher than power contour, which means the vehicle has better acceleration capacity and the factor x is tend to be a smaller one. But for this question, Ref. [12] has a contrary statement. While x equals to different values, from Eq. (1.7) it can be concluded that it is a curve of exponential function a^x. When a is smaller than 1, the smaller x is, the larger the value of exponential will be, which means the velocity is higher. The conclusion is verified by comparing simulation curves shown in Fig. 1.18.

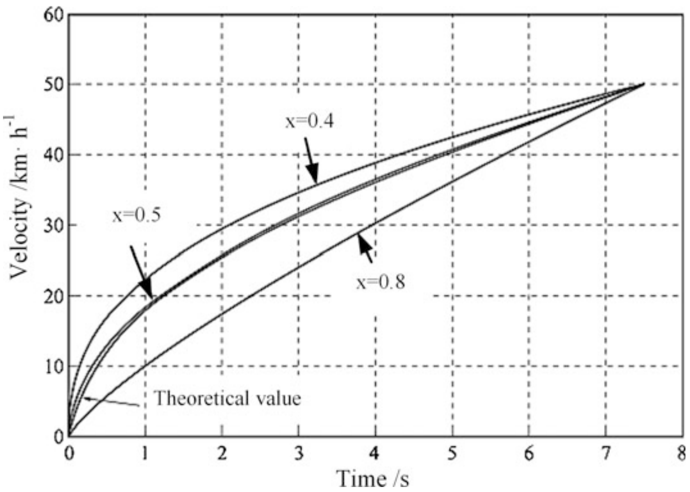

Fig. 1.18 Comparison of acceleration fitting curves

Through the above derivation and comparison, the following conclusions can be drawn:

The fitting factor x is 0.5, which is assumed that the power source is ideal and ignores the rolling resistance and air resistance.

For the actual conditions:

(1) When taking resistance into account, velocity increases slowly. So fitting factor $x > 0.5$, the bigger x is, the bigger vehicle resistance will be.
(2) While not considering about resistance, or for the dynamic stronger vehicle, its external characteristics is higher than power contour and fitting factor $x < 0.5$. So the smaller x is, the stronger vehicle dynamic will be. Reference [12] has a wrong statement about this.

1.2.2.4 Total Power Demand

According to acceleration theoretic equations above, a method to solve total power of power source based on acceleration index can be got. Assuming that vehicle accelerates on a flat road, based on vehicle acceleration kinetic equation, transient power is:

$$P_{total} = P_j + P_f + P_w = \frac{1}{3600 \cdot \eta_t}\left(\delta \cdot m \cdot v\frac{dv}{dt} + m \cdot g \cdot f \cdot v + \frac{C_D \cdot A}{21.15}v^3\right) \quad (1.8)$$

where P_{total} is total power of acceleration process, P_j is power of acceleration and δ is rotational mass conversion factor.

Because the maximum power is assumed to equal power, the average power output during the acceleration process is equal to the maximum power of the power source.

$$
\begin{aligned}
P_{total} &= \frac{W}{t_m} = \frac{\int_0^{t_m} (P_j + P_f + P_w)dt}{t_m} \\
&= \frac{1}{3600 \cdot t_m \cdot \eta_t} \left(\delta \cdot m \cdot \int_0^{v_m} v dv + m \cdot g \cdot f \cdot \int_0^{t_m} v dt + \frac{C_D \cdot A}{21.15} \int_0^{t_m} v^3 dt \right)
\end{aligned}
\tag{1.9}
$$

Make $v = v_m(t/t_m)^{0.5}$ and substitute it into equation above:

$$
P_{total} = \frac{1}{3600 \cdot t_m \cdot \eta_t} \left(\delta \cdot m \cdot \frac{v_m^2}{2} + m \cdot g \cdot f \cdot \int_0^{t_m} v_m \left(\frac{t^{0.5}}{t_m^{0.5}} \right) dt + \frac{C_D \cdot A}{21.15} \int_0^{t_m} v_m^3 \left(\frac{t^{1.5}}{t_m^{1.5}} \right) dt \right)
\tag{1.10}
$$

Simplify it as

$$
P_{total} = \frac{1}{3600 \cdot t_m \cdot \eta_t} \left(\delta \cdot m \cdot \frac{v_m^2}{2} + m \cdot g \cdot f \cdot \frac{v_m}{1.5} \cdot t_m + \frac{C_D \cdot A \cdot v_m^3}{21.15 \times 2.5} \cdot t_m \right)
\tag{1.11}
$$

The first term is the main part of vehicle power, which is power of acceleration. Generally, the power of acceleration is much larger than the other two terms.

1.2.3 Application of Power Calculation Method

1.2.3.1 Assumption of External Characteristics

To explain whether the theoretical equation can be used in the design of the total power of vehicle power source, it is assumed that there is a driving motor, whose external characteristics is close to power contour. But for the real power source, it's impossible to meet the power contour. For example, an EV has a driving motor whose external characteristics is close to power contour as its power source, after matching a multi-shift transmission, power source will be much closer to power contour and its external characteristics curve is shown in Fig. 1.19.

According to the external characteristics of this power source, the theoretical calculation and simulation are carried out respectively. Respectively, as for considering and not considering other resistances of acceleration process, different calculation methods to calculate the vehicle total power are compared.

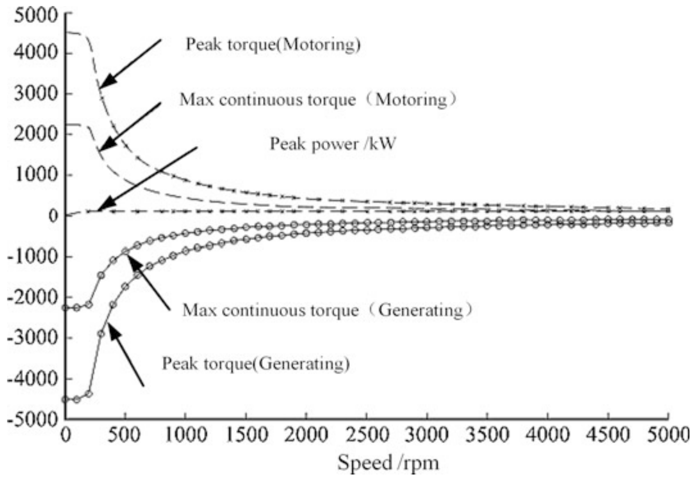

Fig. 1.19 External characteristics curve

1.2.3.2 Comparison of Simulation and Theoretical Results

The vehicle uses the power source close to the above power contour. Comparison of simulation curve, theoretical integration acceleration curve and fitting curve are shown in Fig. 1.20.

It can be seen that the above acceleration curves fit well, especially the power contour fitting curve fits the theoretical integration acceleration curve perfectly and they fit well with simulation curve at later period of the acceleration process.

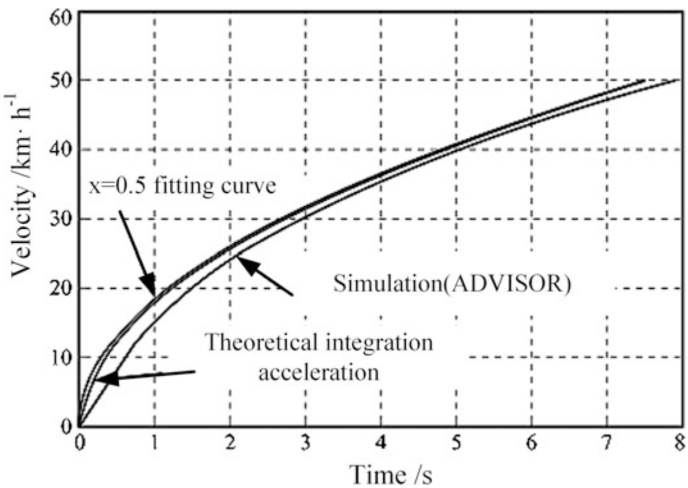

Fig. 1.20 Velocity curves during acceleration

Table 1.15 Acceleration time and deviation

Calculation method	Acceleration time of 0–50 km·h^{-1}/s	Deviation with simulation result/s	Error rate/%
Simulation	7.9	\	\
Fitting curve x = 0.5	7.51	0.39	4.9
Theoretical integration method without resistance	7.51	0.39	4.9
Theoretical integration method with resistance	8.17	0.27	3.4

After adding actual resistance factor into this three curves, which means considering vehicle air resistance and rolling resistance, the acceleration curves and acceleration time are calculated with different methods. Comparison of results are shown in Table 1.15.

These results show that curves from vehicle theory equation fit well with power contour fitting curves. Because both the methods are in a presumed ideal state (i.e., no resistance term is considered), they are slightly different in the initial phase of acceleration and then substantially completely coincide. This is due to the calculation of the vehicle theory method is not fully calculated by power contour, velocity will be smaller when accelerating at low speed.

Theoretical integration calculation has deviation with actual simulation curves. One reason for this deviation is that the simulation process does not ignore the rolling resistance and air resistance. And the other reason is that there is power loss on the ADVISOR platform, which makes acceleration time 7.5 s longer than the theoretical value, which is 7.9 s in simulation. But from comparison of the simulation results, it is indicated that theoretical integration calculation power source can be well fit with the simulation and the deviation is small in the extent permitted.

Now, further study on the influence of considering resistance during the acceleration or not is taken. As shown in Fig. 1.21, the theoretical calculation curve considering resistance fits well with that not considering resistance at low speed. Comparison of driving torque with or without resistance is shown in Fig. 1.22.

It shows that, for the small resistance at low velocity, the two driving torques are close and the curves fit well. Resistance rises as the velocity increases and the curves do not fit very well with each other at high velocity.

After considering the resistance, acceleration curves from theoretical integrate calculation and ADVISOR simulation are very close. Acceleration time of theoretical calculation is 8.17 s, the deviation with ADVISOR simulation result 7.9 s is smaller, just is 3%.

Through the discussion on vehicle acceleration process, the conclusions are as follows: (1) The total power of vehicle is mainly determined by the acceleration process. (2) The acceleration process of vehicle can be simplified as an equal power

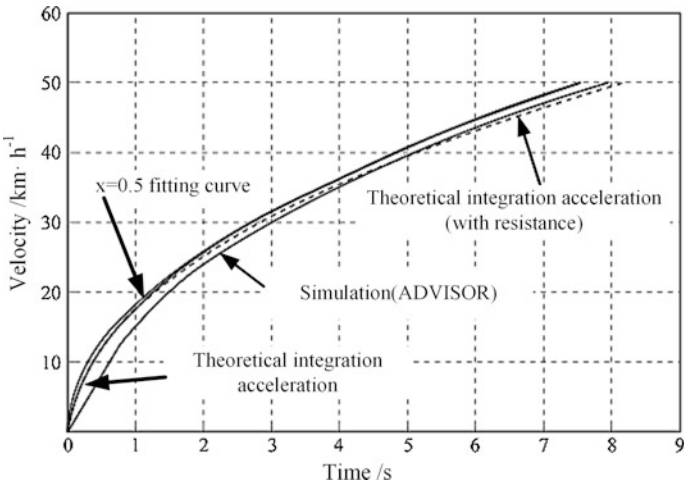

Fig. 1.21 Velocity curves during acceleration

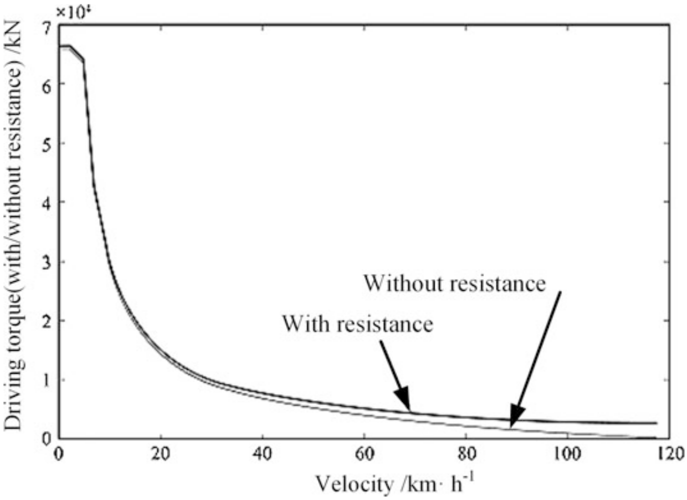

Fig. 1.22 Comparison of driving torque with/without resistance

process. Besides, through the comparison of calculation methods and actual simulation results, it can be seen that the direct curve-fitting method is the intuitive and effective way to calculate the total power, which makes it possible to estimate the total source power with acceleration performance of vehicle. This method can provide practical guidance for the enterprises to design their power source.

1.3 Summary

In this chapter, the actual energy consumption of conventional vehicle is analyzed with visual graphics. It can be concluded that choosing an engine with smaller power, eliminating engine idling and driving in pure electric mode in hybrid vehicle can improve the vehicle efficiency effectively. Then, based on the traditional power calculation method, a solution of directly designing the vehicle power through the acceleration performance index is proposed. After computing the actual simulation calculation, it is verified that the proposed power calculation method is intuitive, effective and accurate when solving the total power demand of the power source.

References

1. Chen Q, Sun F. Hybrid vehicle foundation. Beijing Institute of Technology Press; 2001.
2. Jun Li. The automobile powertrain core technology route and FAW's strategy for environmental protection and energy conservation. Eng Sci. 2009;11(08):64–71.
3. Raymond A, Sutula RA, Heitner KL, Rogers SA, et al. Advanced automotive technologies energy storage R&D programs at the US department of energy-recent achievements and current status. SAE Technical Paper, 2000-01-1604.
4. Hongyan Fang, Jin Wang, Keqiang Liu. Automotive industry energy analysis and energy-saving technology research. Automobile & Parts. 2009;35:42–5.
5. Gao Y, Rahman KM, Ehsani M. Parametric Design of the Drive Train of an Electrically Peaking Hybrid (ELPH) Vehicle. SAE Technical paper; 1997. p. 145–150.
6. Zeng X. Study on mechanism of energy saving and method of parameter design for hybrid electric bus. Jilin University; 2006.
7. Chu L. Control strategy and matching method for hybrid powertrain. Jilin University; 2006.
8. Qingnian Wang, Xiaohua Zeng. The application of hybrid power technology in military vehicles. J Jilin University (Engineering and Technology Edition). 2003;1:38–42.
9. Yu Z. Automotive Theory. China Machine Press; 1982.
10. Liu M. Study on vehicle control strategy and assembly parameter matching for hybrid electric bus. Jilin University; 2005.
11. Andersson T, Groot J. Alternative energy storage system for hybrid electric vehicles. Department of Electric Power Engineering Chalmers University of Technology; 2003.
12. Ng HK, Anderson JL, Santini DJ, Vyas AD. The prospects for electric and hybrid electric vehicles: second-stage results of a two-stage Delphi study; 1996.